

Effect of Sr and Mn co-doping on multiferroic properties of BiFeO₃ via sol-gel chemical process

Sumaiya Jannat, Md. Rafiqul Islam, Ahmed Sharif

Department of Materials and Metallurgical Engineering, Bangladesh University of Engineering and Technology, Dhaka 1000, Bangladesh

Abstract. In this contribution, Sr and Mn co-doped Bi_{0.90}Sr_{0.10}Fe_xMn_{1-x}O₃ (X=0, 5%, 10%, 15%) nanoparticles were prepared by sol-gel (chemical route) method to observe the dominance of co-substitution on their grain size, morphology, UV-vis absorbance and magnetic properties. Co-substitution of Sr and Mn in BiFeO₃, leads to structural transformation from rhombohedral (R3c) to orthorhombic (Pn2₁a). Field emission scanning electron microscope reveals that upon Mn doping nanoparticles become finer. The M-H loops depict that at 15 mol. % Mn doping the saturation magnetization (Ms) is enhanced significantly. Moreover, the synthesized nanoparticles absorb visible light and their band gaps reduce substantially.

Keywords: BiFeO₃, XRD, Morphology, Magnetic properties

1. Introduction

Multiferroics are the compound of having both ferroelectric and magnetic properties and perhaps BiFeO₃ (BFO) is the promising multiferroic material which possesses both of these excellent properties at room temperature. As a result it creates a great field in the application of ferroelectric memories, magnetic tape, nano scale shape memory device, spintronics, and memory device etc. The room temperature structure of BFO is rhombohedral that belongs to point group R3c. It is the only few multiferroics that has Curie (830 °C/1103 K) and Neel (370 °C/643 K) temperatures far above room temperature. [1, 2]

BFO exhibits magneto electric coupling at room temperature and such coupling is strongly influenced by proper doping. However, BFO has some drawbacks in practical application. These are low stability, high leakage current and weak magnetic properties. The rare earth materials like Sr, Ba are doped in the substitution of A-site (Bi) and make the structure more stable, retain the non-Centro symmetry. The transition metal like La, Ni, Ti, Mn, Cr etc are doped in the substitution of B-site (Fe) that minimize the valance fluctuation of Fe³⁺ and compensate the oxygen vacancies [3]. The aim of this synthesis is to investigate the effects of Sr²⁺ and Mn²⁺ doping on the structure, morphology, magnetic properties and uv-vis absorbance.



2. Experimental

Sr and Mn co-doped bismuth ferrites with the composition $\text{Bi}_{0.9}\text{Sr}_{0.1}\text{Fe}_{1-x}\text{Mn}_x\text{O}_3$, where $x = 0$ (BSFMO-0), $x=0.05$ (BSFMO-5), $x=0.10$ (BSFMO-10) and $x=0.15$ (BSFMO-15), nanoparticles were synthesized employing soft chemical sol-gel process at low temperature. In this process the raw materials ($\text{Bi}(\text{NO}_3)_3 \cdot 5\text{H}_2\text{O}$; $\text{Fe}(\text{NO}_3)_3 \cdot 9\text{H}_2\text{O}$; $\text{Sr}(\text{NO}_3)_2$) were weighted respectively in 1:0.95:0.05; 1:0.88:0.05; 1:0.81:0.05; 1:0.76:0.05 ratios. The powders were taken in a beaker and 250 mL de-ionized water was added to make a solution. The solution was heated under stirring on a hot plate at 300 rpm at 200 °C for ½ hr and then required amount of citric acid and ethylene glycol were added to the solution. The solution was heated continuously at 75-80 °C and stirred at 400 rpm until the gel was formed. A vigorous reaction took place to burn the gel. When the reaction was over, the residue was dried in an oven at 120 °C for 18-20 hours. The fluffy powder was obtained by crushing the dried substrates in a mortar. To obtain a crystallized sample the fine powders were further annealed at 500 °C for two hours.

The samples were characterized by X-ray diffraction (XRD using CuK_α radiation model 3040-X'Pert PRO, Philip), field effect scanning electron microscope (FESEM: JEOL JSM 7600F) and energy dispersive X-ray spectroscopy (EDS). Magnetic characterization was performed by using vibrating sample magnetometer (Micro sense easy VSM software version 9.13) & Uv-vis spectroscopy (PerkinElmer UV win lab data Processor and viewer version 1.1.00).

3. Results and discussion

The XRD pattern of the BSFMO-0, BSFMO-5, BSFMO-10 and BSFMO-15 powder samples at RT confirms the formation of crystalline BFO phase (figure-1). The diffraction was performed by using Bragg angles between 20°-90°. Here, the A-site substitute Sr is fixed concentration that is 10%. Pure BFO shows separated diffraction peaks of the (104) & (110) plane. The peak position of (104) plane of pure BFO is situated at 31.72°. But in this case from Fig. (1) It can be seen that the merged peak has a maximum intensity around 31.98 for BSFMO-0 ceramic i.e. the peak shifted to the right with respect to pure BFO. It occurs due to the ionic radius of Sr^{2+} (1.18 Å) is larger than that of Bi^{3+} (1.17 Å) as a result the lattice parameter of BSFMO was increased. [4] Adding Mn^{2+} (5%, 10%, 15%) in substitution of Fe^{3+} shifts the peak to the right because the ionic radius of Mn^{2+} (70 pm) on the other hand Fe^{3+} is 60 pm. The R3c to P_n2_1 a phase transition is found to increase with increasing Mn doping and single P_n2_1 a phase is obtained for BSFMO-15

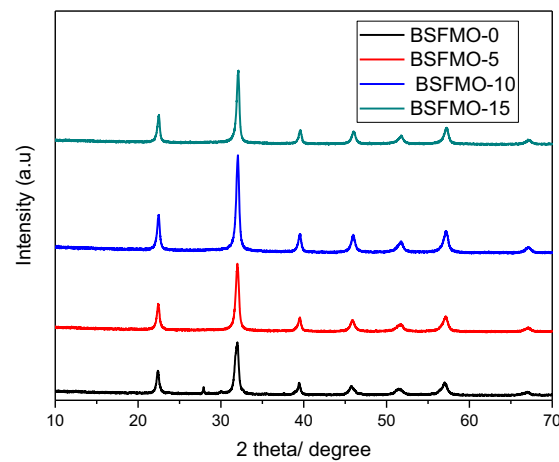


Figure 1. XRD patterns BSFMO-(0, 5, 10 and 15) nanoparticles at room temperature

It is wonder that difference between ionic radii of substituted ions could play a role to modify the crystal structure of BFO.

In BSFMO -0 the surface was irregular, larger grain size and the amount of surface porosity was higher in comparison with other BSFMO ceramics (figure-2).

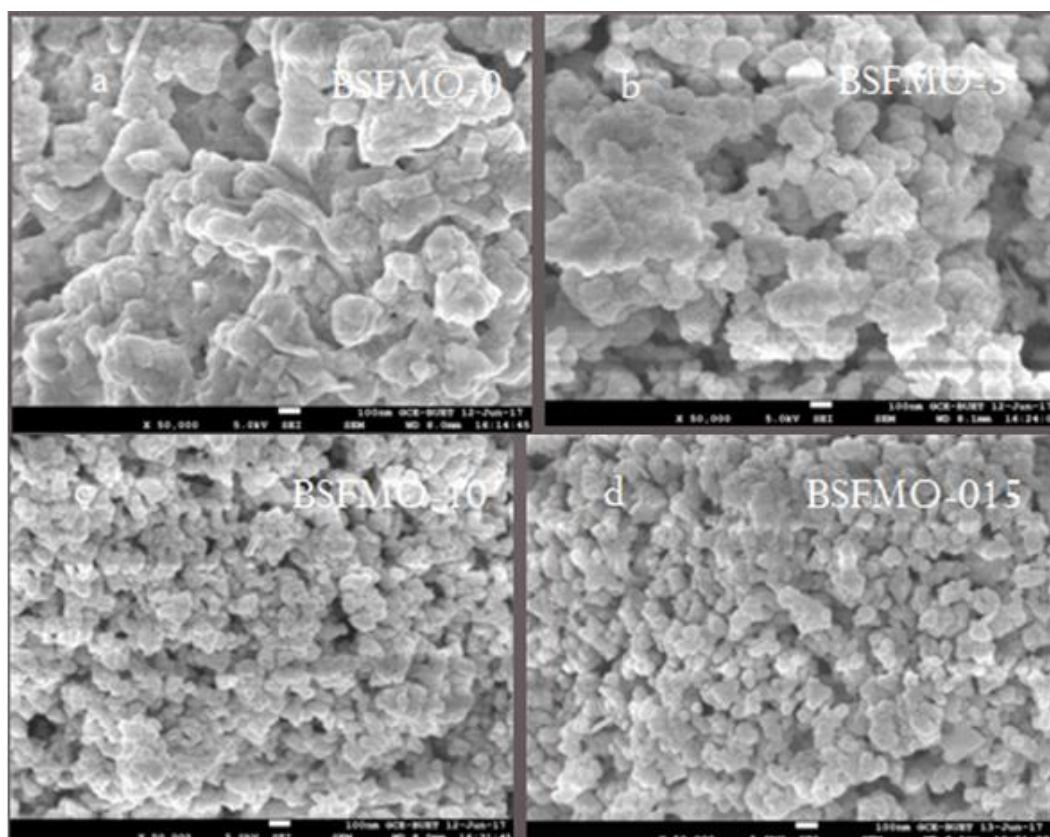


Figure 2. FESEM microstructure of BSFMO nanoparticles (a) BSFMO-0, (b) BSFMO-5, (c) BSFMO-10, (d) BSFMO-15

The higher amount of porosities and rougher surface might arise from the creation of oxygen vacancies in the structure due to hetero-valent substitution of Bi^{3+} with Sr^{2+} in BFO.

The SEM morphology suggests that the grain size and particle size of Sr-Mn co-doped BFO nanoparticles decreases with increasing doping concentrations in $\text{Bi}_{0.90}\text{Sr}_{0.10}\text{Fe}_x\text{Mn}_{1-x}\text{O}_3$ ($X=0, 5\%, 10\%, 15\%$). It clarifies that Sr and Mn both acts as a growth inhibitor. The differences in ionic radii between A-site Bi^{3+} (1.03 Å) to Sr^{2+} (1.18 Å) ion and B-site Fe^{3+} (0.645 Å) to multi valance Mn^{2+} (0.83), Mn^{3+} (0.645 Å), Mn^{4+} (0.53 Å) ions lead to a lattice distortion which hinder crystallite nucleation and thereby reduces particle size [5].

When larger ionic radius Sr^{2+} was doped in A-site it modified the lattice structure of the BFO and suppresses the spiral spin structure. Due to formation of oxygen vacancies the bond angle of $\text{Fe}^{3+}\text{-O-Fe}^{3+}$ could be changed and induce canting of the Fe^{3+} ions spin. The effect of altering the $\text{Fe}^{3+}\text{-O-Fe}^{3+}$ bond angle, rearranged lattice structure with larger ionic replacement and ferromagnetic pinning could produce a net magnetization in the BSFMO-0 structure (figure-3).

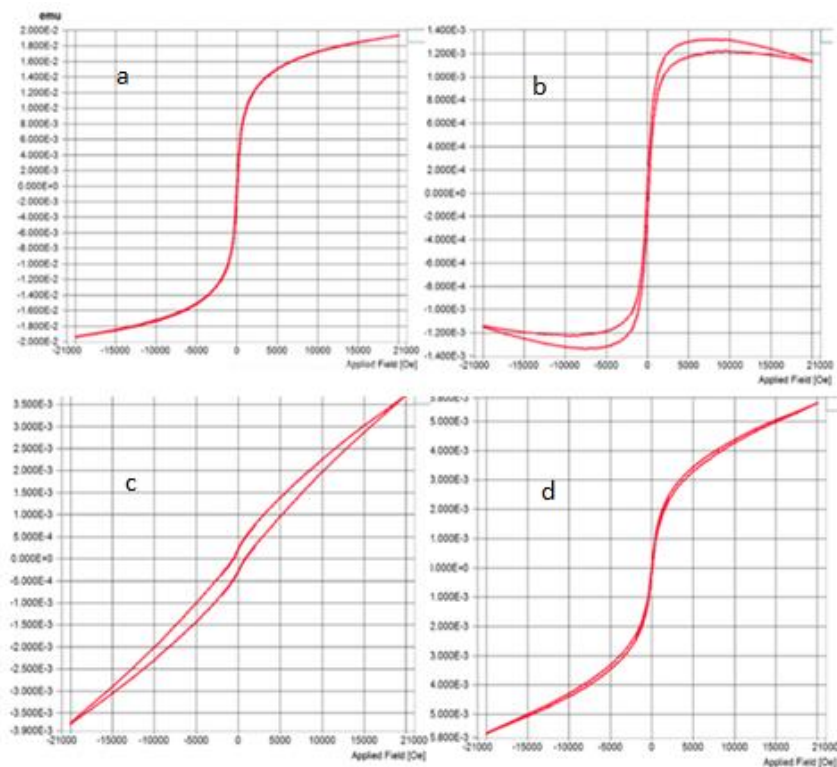


Figure 3. The four figures depict the magnetization vs. applied magnetic field ($M-H$) loops for (a) BSFO, (b) BSFMO-5, (c) BSFMO-10 (d) BSFMO-15 nanoparticles at room temperature.

Addition of Mn^{2+} increases the H_c values and at the last sample it decreases (table-1). Mn^{2+} Magnetic, its magnetic moment of Bohr magneton $\mu_B = 5$. Mn generally stay at multivalent states in BFO and the substitution of Fe^{3+} ([Ar] $3d^5$, $\mu_B = 5$) by Mn^{2+} ([Ar] $3d^5$, $\mu_B = 5$), Mn^{3+} ([Ar] $3d^4$, $\mu_B = 4$) and Mn^{4+} ([Ar] $3d^3$, $\mu_B = 3$) ion may cause incomplete compensation of antiferromagnetic SMSS and onset net magnetization. Furthermore, it was mentioned earlier that Sr and Mn co-doping in BFO has significantly reduced particle size of the synthesized nanoparticles. The suppression of spiral modulated spin structure and contribution of uncompensated spins at the particle surface increases sharply with decreasing particle size of BFO nanoparticles and may lead to the enhanced magnetization with increasing doping concentration.

Table -1: Magnetic parameters of BSFMO-(0, 5, 10, and 15) ceramics at room temperature

Samples	H_c (Oe)	M_r (emu/g) *(e-6)	M_s (emu/g) *(e-3)
BSFMO-0	43.50	948.154	10.39
BSFMO-5	105.17	152.3	1.140
BSFMO-10	695.61	251.46	3.72
BSFMO-15	41.173	118.342	5.63

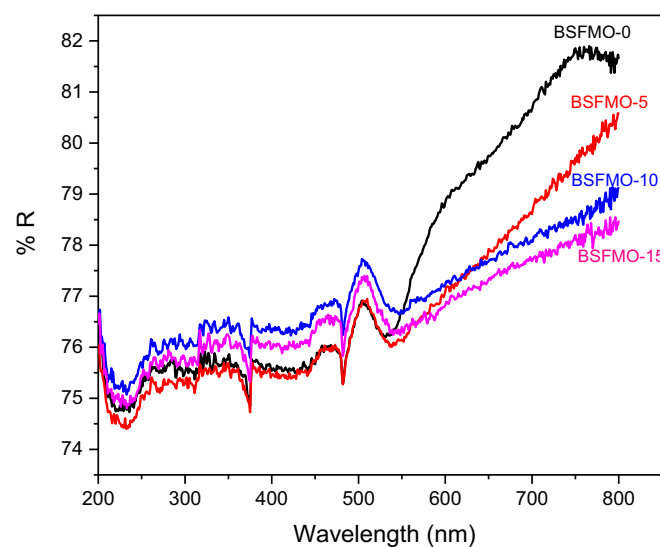


Figure 4. UV-Vis absorption spectra of BSFMO- (0, 5, 10, 15)

BFO is a fascinating optical material which can be used in the application of optoelectronic device. Optical band gap is actually the band gap with energy equals to the energy of visible light. For the pure BFO nanoparticles shows a blue emission around 454 nm and optical band gap is 2.30 eV [6]. But figure 4.

demonstrates that 10% Sr and Mn co-doping has really reduced the optical band gap due to reduced degree of hybridization associated with a stable electronic configuration of Mn^{2+} ($3d^5 4s^0$ half occupation of d orbital) and therefore green emission around 517 nm is seen . Band gap reduces from 2.30 eV to 2.17 eV (green spectrum). The luminescence center as Mn^{2+} ion creates a amount of electron -hole pairs recombination and emits more photons. [7]

4. Conclusion

Structural, magnetic and electrical properties of Sr and Mn co-doped BFO via sol-gel were investigated. sol-gel process has great control over property than other conventional solid state or critical hydrothermal methods. Co-substitution with Sr and Mn leads to structural transformation from rhombohedral (R3c) to orthorhombic ($\text{Pn}2_1\text{a}$) symmetry which was found to have great effect on optical band gap energy, magnetization and electrical conductivity of BFO. In XRD analysis secondary phase was detected though their effect was hardly observed in their properties. Both Mn^{2+} and Sr^{2+} both act as growth inhibitor. oxygen vacancy and charge imbalance created by Sr^{2+} was not adjusted by other charge because Mn^{2+} is also divalent. Thus that leakage current was increased. The magnetic property values of BFO were greatly enhanced due to the size-confinement effects and (Mn , Sr) ions doping. Satisfying ferromagnetic performance was achieved due to the suppression of helical order at room temperature. The improved electric and magnetic properties of the co-doped BFO may be suitable for modern device applications.

Acknowledgements

Author would like to thank Materials and Metallurgical Engineering Department for giving support and also thanks to Glass and Ceramic Engineering department of Bangladesh University of Engineering and Technology.

Reference

- [1]. Gustau Catalan and James F. Scott, Published online: May 4, 2009, Physics and Applications of Bismuth Ferrite Volume 21, pg-2
- [2]. Medina Traya Bismuth-Ferrite-review Bismuth Ferrite review Levy on Feb 21, 2014
- [3]. Xia Yan, Guoqiang Tan, Wenlong Liu, Huijun Ren, Ao Xia Structural, electric and magnetic properties of Dy and Mn co-doped BiFeO_3 thin films (7 november, 2014) School of Materials Science and Engineering, Shaanxi University of Science & Technology, Xi'an, Shaanxi 710021, China
- [4]. Md. Rafiqul Islam, Roisul Hasan Galib , Ahmed Sharif , Mehedi Hasan ,

Md. Abdullah Zubair , Md. Fakhrul Islam ,available 14 july ,2016 Correlation of charge defects and morphology with magnetic and electrical properties of Sr and Ta co-doped BiFeO₃

- [5]. Mehedi Hasan , M.A. Basith , M.A. Zubair, Md. Sarowar Hossain ,Rubayyat Mahbub , M.A. Hakim , Md. Fakhrul Islam Saturation magnetization and band gap tuning in BiFeO₃ nanoparticles via co–substitution of Gd and Mn
- [6]. Xuelian Yu, Xiaoqiang AnEnhanced magnetic and optical properties of pure and (Mn, Sr) doped, BiFeO₃ nano crystals
- [7]. J. F. Ihlefeld, N. J. Podraza, Z. K. Liu,R. C. Rai, X. Xu, T. Heeg Y. B. Chen,J. Li, R. W.Collins,J. L. Musfeldt, X. Q. Pan, J. Schubert,R. Ramesh, and D. G. Schlom, Optical band gap of BiFeO₃ grown by molecular-beam epitaxy published online 10 April 2008